Momentum-dependence of charmonium spectral functions from lattice QCD

Mehmet Buğrahan Oktay[1] and Jon-Ivar Skullerud[2]

[1]*Department of Physics, University of Utah, 115 S 1400 E, Salt Lake City, UT 84112-0830 USA.*
[2]*Department of Mathematical Physics, NUI Maynooth, County Kildare, Ireland.*
(Dated: May 10, 2010)

We compute correlators and spectral functions for J/ψ and η_c mesons at nonzero momentum on anisotropic lattices with $N_f = 2$. We find no evidence of significant momentum dependence at the current level of precision. In the pseudoscalar channel, the ground state appears to survive up to $T \approx 450\text{MeV}$ or $2.1T_c$. In the vector channel, medium modifications may occur at lower temperatures.

I. INTRODUCTION

The survival and properties of charmonium bound states in the quark–gluon plasma is a hot topic in the interpretation of experimental results from relativistic heavy-ion collisions. A variety of models have been put forward to explain the observed pattern of suppression of the J/ψ yield, including sequential suppression [1], charmonium regeneration through coalescence of uncorrelated $c\bar{c}$ pairs [2–4], and combinations of these two mechanisms [5].

Results from lattice simulations [6–9] suggest (though far from decisively [10]) that S-wave ground states (J/ψ and η_c) survive up to temperatures close to twice the pseudocritical temperature T_c, while excited states (ψ') and P-waves (χ_c) melt at temperatures close to T_c, in rough agreement with the sequential suppression scenario. These results are however not sufficient to rule in favour of one or other scenario.

An additional handle on the problem may be gained by considering charmonium states which are moving with respect to the thermal medium. The two main scenarios (regeneration and sequential suppression) predict different transverse momentum and rapidity dependence of the charmonium yield. This is primarily due to the momentum dependence of the reaction rates included in these scenarios, but in order to complete the story it will also be necessary to investigate any momentum dependence of the baseline survival probability of charmonium bound states. This paper provides the first steps in this direction.

The analytical structure of QCD correlators implies that both spatial and temporal correlators are governed by the same spectral function. However, in order to describe spatial correlators and screening masses, it is necessary to also include the spatial-momentum dependence of the spectral function.

Finally, computing spectral functions at nonzero momentum may also facilitate the determination of transport coefficients such as the heavy quark diffusion constant [11], as the zero-frequency transport peak is broadened and shifts to nonzero frequency.

We will work on a spatially isotropic lattice, which means that the anisotropy of the plasma created in heavy-ion collisions is not taken into account. Our momentum is best interpreted as the transverse momentum, and we will therefore not be able to say anything at this point about the rapidity dependence of any observables.

II. FORMULATION

We have simulated two degenerate flavours of $\mathcal{O}(a)$-improved Wilson fermions, with $m_\pi/m_\rho = 0.54$ (corresponding approximately to the strange quark mass), and with spatial lattice spacing $a_s = 0.162\text{fm}$ and anisotropy $\xi = a_s/a_\tau = 6$. The lattice action is described in more detail in Ref. [12], and the high-temperature simulation parameters are discussed in Ref. [13]. Our parameters here correspond to Run 7 in Ref. [13]. The same fermion action is used for both light sea and heavy valence quarks. The lattices, corresponding temperatures and number of configurations N_{cfg} used in this study are given in Table I. The main difference compared to Ref [13] is that all our data are now obtain using the tuned (Run 7) parameters and on a spatial volume of 12^3 in lattice units.

N_s	N_τ	T (MeV)	T/T_c	N_{cfg}
8	80	92	0.42	250
12	80	92	0.42	250
12	32	230	1.05	1000
12	28	263	1.20	1000
12	24	306	1.40	500
12	20	368	1.68	1000
12	18	408	1.86	1000
12	16	459	2.09	1000

TABLE I: Lattice volumes, temperatures and number of configurations used in this simulation. The separation between configurations is 10 HMC trajectories, except for the $N_\tau = 80$ runs where configurations were separated by 5 trajectories. The lattice spacings are $a_s \sim 0.162\text{fm}$, $a_\tau \simeq 7.35 \pm 0.03\text{GeV}$.

Spectral functions were computed using the maximum entropy method as described in [13], with the modified kernel introduced in Ref. [14]. The charmonium correlators were computed using all-to-all propagators with dilution in time, color and varying levels in space and spin. The momentum values are given by
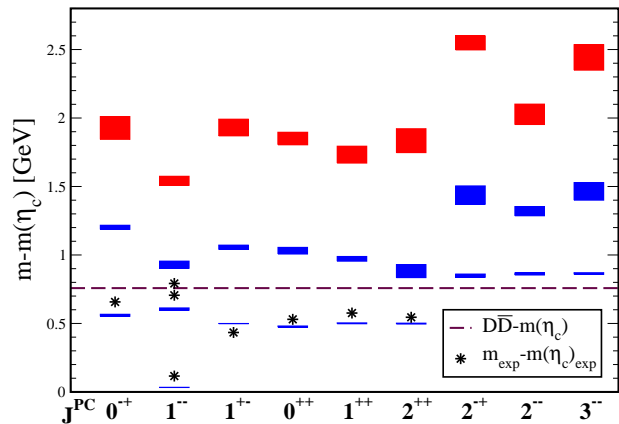
FIG. 1: The mass splittings of the low-lying charmonium spectrum at zero temperature, with the known experimental values and the $D\bar{D}$ threshold also indicated.

J^{PC}	$^{2S+1}L_J$	State	Operators
0^{-+}	$^1S_0$	η_c, η_c'	$\gamma_5, \gamma_5 \sum_i s_i$
1^{--}	$^3S_1$	$J/\Psi, \Psi(2S)$	$\gamma_j, \gamma_j \sum_i s_i$
1^{+-}	$^1P_1$	h_c, h_c'	$\gamma_i\gamma_j, \gamma_5 p_j$
0^{++}	$^3P_0$	χ_{c_0}, χ_{c_0}'	$1, \vec{\gamma}\cdot\vec{p}$
1^{++}	$^3P_1$	χ_{c_1}, χ_{c_1}'	$\gamma_5\gamma_i, \vec{\gamma}\times\vec{p}$
2^{++}	$^3P_2$	χ_{c_2}, χ_{c_2}'	$\vec{\gamma}\times\vec{p}, \gamma_1 p_1 - \gamma_2 p_2$
			$2\gamma_3 p_3 - \gamma_1 p_1 - \gamma_2 p_2$
2^{-+}	$^1D_2$	1^1D_2	$\gamma_5(s_1 - s_2), \gamma_5(2s_3 - s_1 - s_2)$
2^{--}	$^3D_2$	1^3D_2	$\gamma_j(s_i - s_k), \gamma_1 t_1 - \gamma_2 t_2$
			$2\gamma_3 t_3 - \gamma_1 t_1 - \gamma_2 t_2$
3^{--}	$^3D_3$	1^3D_3	$\vec{\gamma}\cdot\vec{t}$

TABLE II: Operator basis used to obtain the $T = 0$ charmonium spectrum. The definitions of s_i, p_i and t_i are given in Ref. [18].
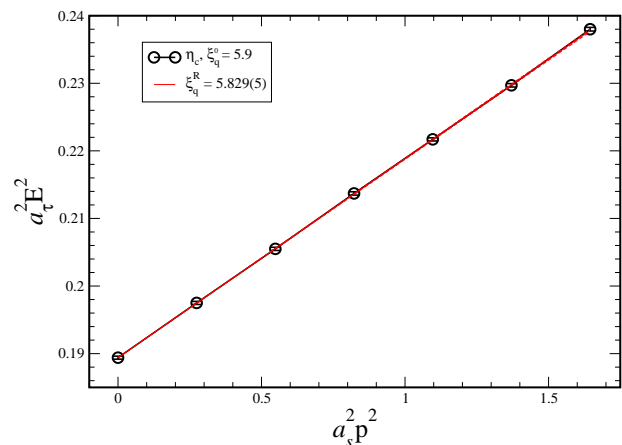
$p^2 = \left(\frac{2\pi}{a_s N_s}\right)^2 n^2$, with $n^2 = 0, 1, 2, 3, 4$, corresponding to $p = 0, 0.66, 0.93, 1.14, 1.32$ GeV. We consider only the pseudoscalar (η_c) and vector (J/ψ) channels. Our correlators have not been renormalised, so the vertical scale on the figures presented is arbitrary, but the shape of the curves is not.

III. RESULTS

A. Zero-temperature spectrum

In order to establish a baseline for our high-temperature results, we first present results for the spectrum and dispersion relation at zero temperature. Taking advantage of the all-to-all propagators, we used the variational method [15, 16] with a large basis of interpolating operators to compute the low-lying spectrum of S-, P- and D-waves. This is shown in Fig. 1, along with the experimentally known masses. The operator basis used in the spectrum study is summarized in Table II. Taking the difference between the spin-averaged 1S masses and the $^1P_1(h_c)$ mass to set the scale, we find the inverse lattice temporal lattice spacing to be $a_\tau^{-1} = 7.35(3)$GeV[19]. In Figure 1 the highest lying radial excitations in each channel are colored red to indicate that they are contaminated by higher excited states. The difference between our results and experiment is largely due to the fairly coarse spatial lattice spacing used. Including a clover term in the action has been found to improve the agreement with experiment [17].

Figure 2 shows the ground-state pseudoscalar (η_c) dispersion relation. The bare anisotropy for the valence charm quarks is $\xi_0^c = 5.90$, which on the $8^3 \times 80$ lattice had given a renormalised anisotropy of 6. However, on the larger ($12^3 \times 80$) lattice we find that the dispersion relation gives us a renormalised anisotropy of 5.829 ± 0.05, giving rise to a 3% systematic error in our final results.

FIG. 2: The η_c dispersion relation.

B. High-temperature spectral functions

In order to facilitate comparisons between spectral functions at different temperatures and momenta, we have determined the spectral functions $\rho(\omega, \vec{p}; T)$ at all T and $\vec{p}$ using the *same* default model, $m(\omega) = m_0\omega^2$ with $a_\tau m_0 = 6$ and $a_\tau m_0 = 4$ for the pseudoscalar and vector channel respectively. These values are close to the 'best' values determined from a one-parameter fit of the correlator for each temperature and momentum considered. We have repeated the analysis for a range of different default models to study the robustness of our results.

As in Ref. [13], the first two timeslices were discarded in the analysis since these will be dominated by lattice artefacts. The effect of varying the time range has also been investigated.

Figure 3 shows the spectral function in both channels at zero momentum for the various temperatures. These results may be compared to Figs. 5 and 6 in Ref. [13]. In the pseudoscalar channel, our results suggest that the
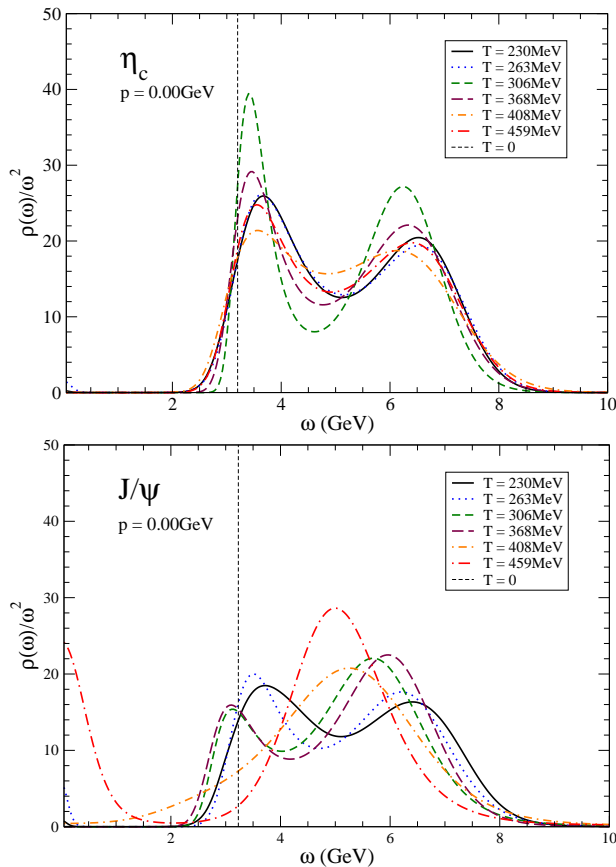
FIG. 3: The pseudoscalar (top) and vector(bottom) spectral function at zero momentum for various temperatures.

FIG. 4: The pseudoscalar spectral function at nonzero momentum for $T = 230$ MeV, using timeslices 2–16 (top) and 3–16 (bottom). The zero-temperature energy levels are also shown for comparison.

ground state (η_c) survives up to the highest temperatures accessible in our simulations, while the J/ψ (vector state) appears to dissolve for $T \gtrsim 370$MeV or $1.7T_c$. It must be noted, however, that the uncertainty in the MEM procedure increases as the temperature increases, and it is therefore not possible at present to say for certain whether the pattern observed at the highest temperatures is genuine or merely reflects the inability of the MEM algorithm to determine the spectral function given the available data. This remains the case for all momenta and in all channels.

Figure 4 shows the pseudoscalar spectral function for different momenta at $T = 230$ MeV. Using $\tau_{\min} = 3$ (lower panel), we see a clear structure of peaks ordered by momentum, with the separation between the peaks corresponding reasonably well to the zero-temperature energy levels. The peak positions, however, appear to be shifted compared to the zero-temperature energies. This is most likely due to the maximum entropy method not being able to resolve the full detail of the spectral function for the available data. This is supported by the upper panel of Fig. 4, showing the spectral functions determined using $\tau_{\min} = 2$. Here the peak position for the lowest non-zero momentum corresponds precisely to the zero-temperature energy, while for the other momenta
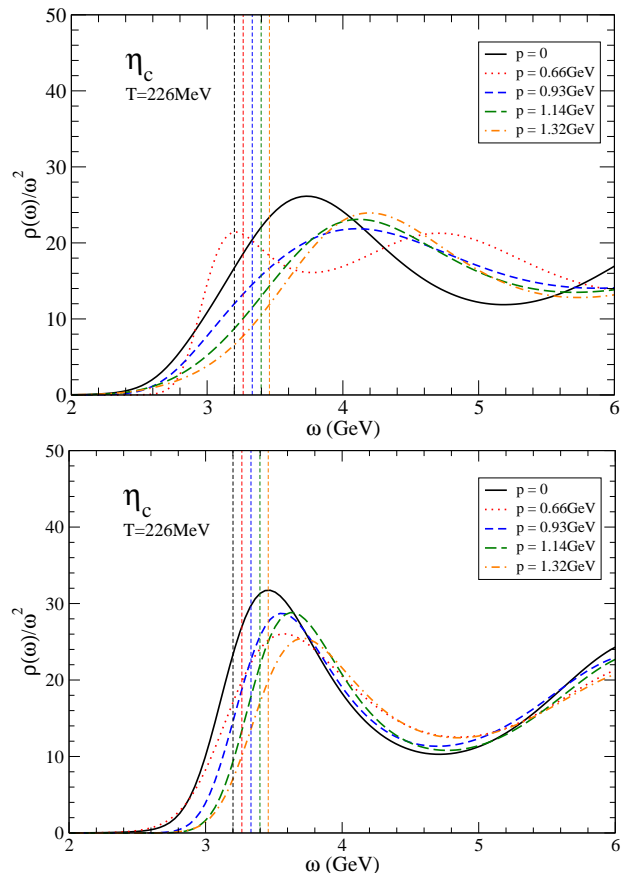
the peaks are smeared out and shifted to higher energies.

Figure 5 shows the pseudoscalar spectral function for different momenta at two higher temperatures. There is still some evidence of a surviving ground state peak at all momenta, but uncertainties in the MEM reconstruction means that we are no longer able to resolve the ordering of the states given our current precision.

At nonzero momentum, the vector meson correlator is decomposed into transverse and longitudinal polarisations,

$$V_{ij}(\tau, \vec{p}) = \left(\delta_{ij} - \frac{p_i p_j}{p^2}\right) V_T(\tau, \vec{p}) + \frac{p_i p_j}{p^2} V_L(\tau, \vec{p}). \quad (1)$$

The transversely and longitudinally polarised J/ψ may in principle behave differently in the medium. We have therefore analysed the two separately. Figures 6 and 7 show the transverse and longitudinal spectral functions for our largest and smallest momentum, respectively. The longitudinal spectral function for the lowest momentum ($p = 0.66$GeV) shows clear evidence of a surviving peak corresponding to the J/ψ ground state at the two lowest temperatures, but there are indications of medium modifications already at $T = 300$MeV. The
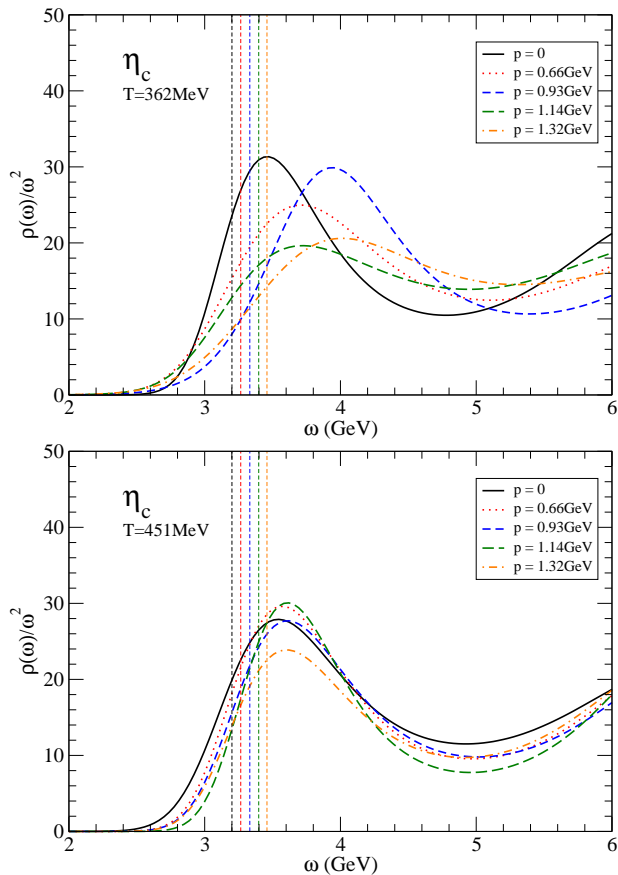
FIG. 5: The pseudoscalar spectral function at nonzero momentum for $T = 368$ MeV (top) and $T = 459$ MeV (bottom). The zero-temperature energy levels are also shown for comparison.

transverse spectral function, on the other hand, appears to be subject to medium modifications (indicated by the softer ground state peak) already at the lowest temperature, just above T_c.

It is worth emphasising that the transverse spectral function at $T = 230$MeV, $p = 0.66$GeV displays little or no sensitivity to the choice of model function, so we consider our result in this case to be robust. At higher momenta and temperatures, the MEM reconstruction of spectral functions is no longer stable with regard to variations in the model function and time range used. Our results for both transverse and longitudinal J/ψ at $p = 1.32$GeV should therefore be taken as no more than indicative, even at the lowest temperature. With this proviso, the indications are that the longitudinal J/ψ survives at least up to 265MeV ($1.2T_c$) and is most likely melted by $T = 400$MeV, while the transversely polarised

J/ψ may experience medium modifications already close to T_c.

IV. DISCUSSION

We have presented first results for charmonium spectral functions at nonzero momentum. Our results suggest that the 1S pseudoscalar meson (η_c) survives up to temperatures close to twice the pseudocritical temperature of QCD, for all momenta. No substantial momentum dependence was found.

In the vector channel, there appears to be a distinction between the transverse and longitudinal channels, with the longitudinally polarised J/ψ experiencing smaller medium modifications. Again, no substantial momentum dependence was found, although the reconstruction of the spectral function became progressively more uncertain with increasing momentum. Therefore, some additional momentum dependence can not be ruled out.

Whether the difference between transverse and longitudinal polarisations is real or merely a reflection of the uncertainty in the MEM procedure given the data used in this study, still needs to be determined.

We are in the process of generating configurations with smaller lattice spacing. This will provide greater temporal resolution, leading to a more reliable determination of spectral functions from imaginary-time correlators. The finer lattice is also expected to bring the zero-temperature spectrum in closer agreement with experiment, and allow a clearer separation between physical features and lattice artefacts in our spectral functions. It will also allow us to access higher temperatures, where all model studies up to now have found the charmonium ground states to be dissolved.

We are also computing correlators of the conserved vector current, which will provide the correct nonperturbative renormalisation of the vector operator used in this study, and permit a quantitative determination of the charm quark diffusion rate and the charmonium contribution to the dilepton rate.

[1] F. Karsch, D. Kharzeev and H. Satz, Phys. Lett. **B637**, 75 (2006), [hep-ph/0512239].

[2] P. Braun-Munzinger and J. Stachel, Phys. Lett. **B490**, 196 (2000), [nucl-th/0007059].
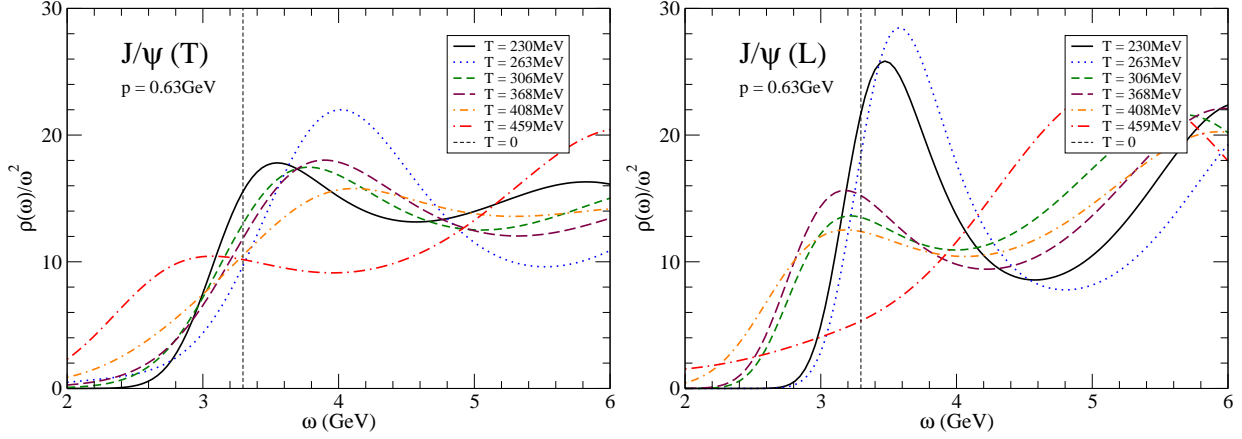
FIG. 6: The transverse (left) and longitudinal (right) vector meson spectral function at $p = 0.66$GeV for various temperatures.

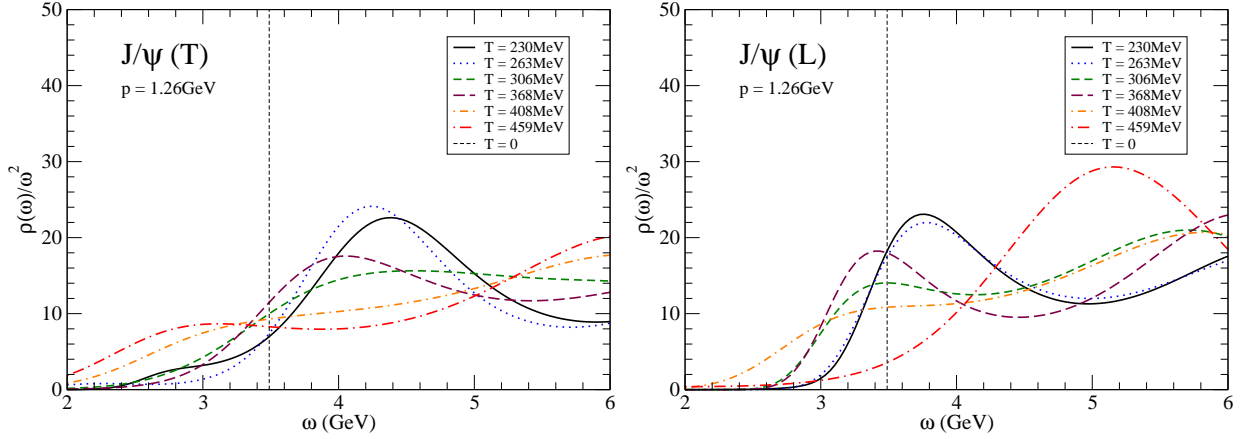FIG. 7: The transverse (left) and longitudinal (right) vector meson spectral function at $p = 1.32$GeV for various temperatures.

[3] R. L. Thews, M. Schroedter and J. Rafelski, Phys. Rev. **C63**, 054905 (2001), [hep-ph/0007323].

[4] R. L. Thews and M. L. Mangano, Phys. Rev. **C73**, 014904 (2006), [nucl-th/0505055].

[5] L. Grandchamp and R. Rapp, Nucl. Phys. **A709**, 415 (2002), [hep-ph/0205305].

[6] T. Umeda, K. Nomura and H. Matsufuru, Eur. Phys. J. **C39S1**, 9 (2005), [hep-lat/0211003].

[7] M. Asakawa and T. Hatsuda, Phys. Rev. Lett. **92**, 012001 (2004), [hep-lat/0308034].

[8] S. Datta, F. Karsch, P. Petreczky and I. Wetzorke, Phys. Rev. **D69**, 094507 (2004), [hep-lat/0312037].

[9] A. Jakovac, P. Petreczky, K. Petrov and A. Velytsky, Phys. Rev. **D75**, 014506 (2007), [hep-lat/0611017].

[10] A. Mocsy and P. Petreczky, arXiv:0705.2559 [hep-ph].

[11] P. Petreczky and D. Teaney, Phys. Rev. **D73**, 014508 (2006), [hep-ph/0507318].

[12] R. Morrin, A. Ó Cais, M. Peardon, S. M. Ryan and J.-I. Skullerud, Phys. Rev. **D74**, 014505 (2006), [hep-lat/0604021].

[13] G. Aarts, C. Allton, M. B. Oktay, M. Peardon and J.-I. Skullerud, Phys. Rev. **D76**, 094513 (2007), [arXiv:0705.2198 [hep-lat]].

[14] G. Aarts, C. Allton, J. Foley, S. Hands and S. Kim, Phys. Rev. Lett. **99**, 022002 (2007), [hep-lat/0703008].

[15] M. Lüscher and U. Wolff, Nucl. Phys. **B339**, 222 (1990).

[16] C. Michael, Nucl. Phys. **B259**, 58 (1985).

[17] S. M. Ryan, private communication.

[18] UKQCD, P. Lacock, C. Michael, P. Boyle and P. Rowland, Phys. Rev. **D54**, 6997 (1996), [hep-lat/9605025].

[19] This replaces the value 7.23GeV reported in Ref. [13], which was obtained using preliminary values for the 1S and 1P masses. Our final values for the η_c and J/ψ masses are also slightly too high as a result.